Article Identifier
DOI: 10.22032/dbt.58695
URN: urn:nbn:de:gbv:ilm1-2023isc-104:5

60th ILMENAU SCIENTIFIC COLLOQUIUM
Technische Universität Ilmenau, 4 – 8 September 2023
URN: urn:nbn:de:gbv:ilm1-2023isc:1

RESOLUTION ENHANCEMENT IN FABRY-PEROT INTERFEROMETERS THROUGH EVALUATION OF MULTIPLE REFLECTION USING RANGE-RESOLVED INTERFEROMETRY

Vitalii Shmagun, Uwe Gerhardt, Eberhard Manske, Thomas Fröhlich, Thomas Kissinger

Institute of Process Measurement and Sensor Technology, Technical University of Ilmenau, Ehrenbergstraße 29, 98693 Ilmenau, Germany

ABSTRACT

This work presents a novel approach for improving interferometer resolution with a relatively simple setup by combining the use of range-resolved interferometry and a high-finesse Fabry-Perot setup utilizing multiple reflections in the cavity to gradually increase the resolution. This approach could enable the measurement of small displacements with a potentially much higher resolution than current interferometry methods. A simple proof-of concept setup demonstrated the evaluation of up to four Fabry-Perot passes, while theoretically much higher sensitivity improvement factors should be possible.

Keywords: Fabry-Perot Interferometer, Range-resolved Interferometry, displacement measurement

1. INTRODUCTION

Interferometers play a crucial role in many scientific and industrial applications that demand high-precision displacement measurements. The Michelson interferometer, the simplest interferometer setup, can achieve sub-nanometer resolution through the interpolation of the interference signal. It has an interferometer factor of 2, which implies that a 2π interference phase advance corresponds to a displacement of half the wavelength. Several methods have been developed to enhance the resolution of interferometers, such as increasing the interferometer factor using more complex optical setups [1], utilizing heterodyne interferometry, and advanced digital signal processing. Impressive achievements in position measurements have been reported [2], demonstrating interferometer resolution of a few pm and periodic nonlinearities of an amplitude smaller than 5 pm. Nonetheless, achieving such high resolution levels necessitates a complicated setup comprising advanced optical, electronic, and mechanical components. In addition, sophisticated alignment procedures are typically required.

With recent advancements in telecommunications technology, the accessibility and use of highly coherent laser diodes in various interferometer setups have significantly increased. Laser diodes, notable for their long lifetime, high output power, and capacity for direct laser frequency modulation via laser injection current modulation, are progressively supplanting conventional laser sources. Direct frequency modulation facilities the application of pseudo-heterodyne phase demodulation techniques, reducing the complexity of the optical interferometer setup by negating the need for a second optical quadrature signal. An emergent technique in this field, range-resolved interferometry (RRI) [3], allows for the separation and concurrent demodulation of multiple interference sources with different optical path differences (OPD) within a single photodetector signal, delivering phase demodulation with low-nonlinearities and allowing

novel interferometer configurations. The capability of RRI-method to independently demodulate interferometers with different OPDs is utilized in this work to enhance the interferometer factor and thereby improve the interferometer resolution.

The method we propose in this work combines the use of range-resolved interferometry (RRI) with a high-finesse Fabry-Perot setup utilizing multiple reflections in the cavity to gradually increase the resolution. The approach should enable the measurement of small displacements with a potentially much higher resolution than what is currently possible with conventional interferometry. This work presents the first experimental demonstration of the principle and confirms that the signals from multiple reflections can be separated in this way. The results demonstrate the principle feasibility of the proposed method for improving interferometer resolution, opening up new possibilities for ultra-precise measurements in various fields of science and engineering.

2. THEORY

The RRI-method utilizes sinusoidal frequency modulation of a laser diode with a large extraction, requiring a laser diode with optical frequency tunable in wide-range (>10 GHz). A comprehensive theory of the RRI-method is detailed in [3] and examples of its application are published in [4, 5, 6]. In this paper, a concise simplified theoretical summary relevant for this study will be presented.

The photodetector signal, $U(t)$, originating from N component interferometers that make up an optical signal, each characterized by a distinct OPD with a corresponding time-of-flight t_n, can be represented as follows:

$$U(t) = I_{avg} + \sum_{n=1}^{N} I_n \cos\{A_n \sin[\omega_m(t - 0.5\tau_n)] + \varphi_n(t)\},$$

where ω_m is the modulation angular frequency, $\varphi_n(t)$ is the desired interference phase, I_{avg} is the average intensity of the photodetector signal, and I_n denotes the sum of the intensity of the two arms forming each individual interferometer, along with their mutual interferometric visibility. A_n is the modulation index, also referred to as the phase carrier amplitude in reference [3], and signifies the amplitude of the phase modulation waveform resulting from the applied optical frequency modulation for a specified OPD. A_n is proportional to the optical modulation amplitude of the laser and to the time-of-flight t_n between the n-th set of interferometer arms.

In this technique, a complex time-variant demodulation phase carrier, $C(t)$, is used for the phase demodulation of each constituent interferometer. This carrier is chosen to approximately match with the phase modulation waveform resulting from the applied sinusoidal optical frequency modulation, and $C(t)$ is given by:

$$C(t) = \exp[\mathrm{j}A_d \sin[t - 0.5t_d]].$$

Here, the demodulation phase carrier amplitude A_d and the demodulation time-of-flight delay t_d are selected to approximate the A_n and τ_n of the n-th interferometer that needs to be evaluated. After multiplying the photodetector signal with the demodulation phase carrier function and applying a Gaussian periodical window function – which is used to suppress the crosstalk components from other interferometers present in the signal, as described in theory in [3], – and applying a low-pass filter to the resulting function, we obtain:

$$Q(t) = \exp\{-\mathrm{j}\varphi_n(t)\}.$$

Consequently, $\varphi_n(t)$ can be retrieved using an arctan function on the $Q(t)$ signal. Retrieved phase signal $\varphi_n(t)$ corresponds to the phase change of the n-th interferometer and it remains unaffected by the phase shifts in other interferometers that have different OPDs in the optical signal. Therefore, RRI method allow for novel optical configuration, where in a single optical beam several interferometers with different OPDs can be multiplexed.

The interferometer optical configuration used in this study is presented in figure 1. It involves a collimated laser beam exiting a fiber and passing through a Fabry-Perot cavity. The light exiting the fiber undergoes Fresnel reflection, and thus part of the light (approximately 4%) is reflected back into the fiber. The remaining part is collimated and enters the Fabry-Perot cavity, where the first mirror reflects part of the signal back and the rest enters the cavity, where it passes the cavity $i = 1..N$ times. After each pass of the cavity from the entrance mirror to the end mirror and back, part of the light exits the cavity and re-enters the fiber. The optical signal propagating back through the fiber is comprised of numerous interference signals, generated by all reflections within the optical setup interfering with each other, composing a complex signal that can nevertheless be evaluated with the RRI method.

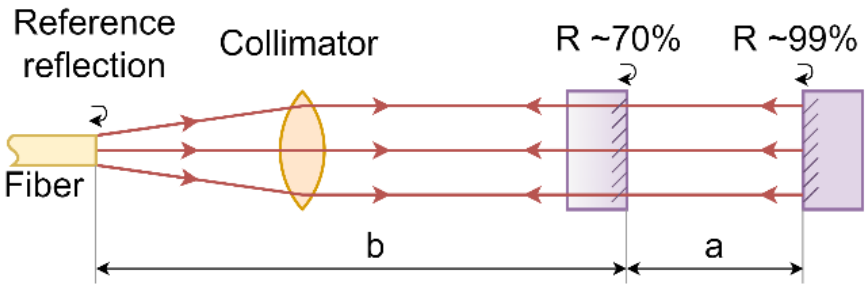

Figure 1. Interferometer optical configuration. Each surface where light is reflected is indicated by a returning arrow.

The interference phases of interferometers at $i \cdot a$ OPD formed entirely within the Fabry-Perot cavity cannot be evaluated directly due to the overlapping of multi-reflection beams. Although they should have nominally the same phase change, evaluating several different interferometers at the same OPD with the RRI method would lead to large nonlinearity error if the refection ratios of the individual interferometers would change. Therefore, a fiber tip reflection is used as a reference and only the constituent interferometers where one interferometer arm is provided by this reference reflection are evaluated. This allows for the unambiguous separation of the signals for the Fabry-Perot passes and thus prevents nonlinearity in phase demodulation.

The interference phase changes of the i-th multi-reflection $\Delta\varphi_i$ can be split into two parts, one for the path before the Fabry-Perot cavity with length b, and the other for the resonator length being measured with length a:

$$\Delta\varphi_i(t) = \Delta\varphi_b(t) + i \cdot \Delta\varphi_a(t).$$

Therefore, for a stable setup with $\Delta\varphi_b\ (t) = 0$, the change of length cavity Δa can be expressed as

$$\Delta a_i(t) = \frac{\varphi_i(t)}{i} \cdot \frac{\lambda_0}{4\pi n},$$

where λ_0 is the laser vacuum wavelength, and n is the refractive index in the cavity. Since the phase change of the interference between the fiber end and the entry mirror $\Delta\varphi_b(t)$ can be also measured with the RRI method, this phase change can be subtracted from the $\Delta\varphi_i(t)$, leaving only the desired phase change of the cavity $i \cdot \Delta\varphi_a(t)$. Therefore, this methodology enables the

evaluation of each i-th iteration of light passage through the cavity. In theory, with every subsequent pass, the factor of the interferometer increases by 2, resulting in a total factor of $k = i * 2$.

To provide the correct scaling and reduce the impact of phase noise, the N available signals can also be summed and then averaged using the total number of Fabry-Perot cavity passes contained within the sum signal.

3. EXPERIMENTAL SETUP

Figure 2 illustrates the experimental configuration. The RRI interrogation unit is equipped with a data acquisition board (low-cost Nucleo-H743ZI2 board from STMicroelectronics) that generates the modulation signal for the laser controller (6305 ComboSource from Arroyo Instruments) and receives the signal from the photodetector (InGaAs Amplified Photodetector PDA05CF2 from Thorlabs). Light from the telecom laser diode (EP1550-0-DM-B01-FA from Eblana Photonics) passes the circulator to the optical setup, and the returning light from the setup is directed back to the photodetector. The length b between the fiber end and the entry mirror is deliberately set to be substantially greater than the cavity length a. This configuration is implemented to avoid overlap between the interferometers created solely within the cavity with an optical path difference (OPD) of $i \cdot a$, and those established in conjunction with the reference exhibiting an OPD of $b + i \cdot a$.

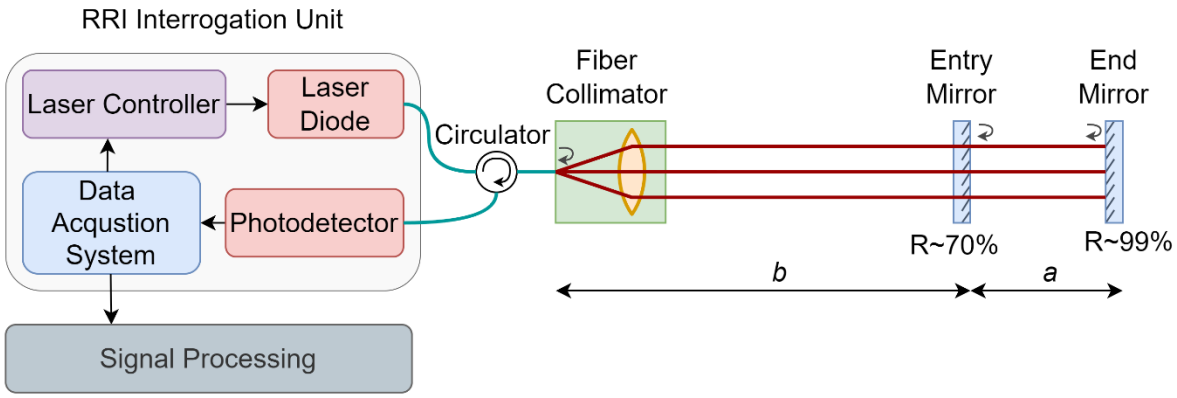

Figure 2. Experimental setup.

Figure 3 presents the photodetector signal obtained from the experimental setup over one modulation period. The RRI method facilitates the computation of a tomographic representation of the optical signal, which shows the correlation between the interference amplitude and the demodulation phase carrier amplitude, revealing each interference source at the corresponding OPD presented in the optical signal. A comprehensive theoretical exposition and explanation on how to derive such a tomographic view, as well as the conversion of demodulation phase carrier amplitude into OPD, can be found in [7]. Figure 4 shows the extracted range dependency of the experimental setup determined by the RRI method. The peaks in this figure are annotated with letters that represent the OPD of the corresponding interferometer. As described in Section 2, only the peaks formed with the reference path b are evaluated for the phase demodulation. For example, phase change $\Delta\varphi_2(t) = \Delta\varphi_b(t) + 2 \cdot \Delta\varphi_a(t)$ corresponds to interferometer with an OPD of $b + 2a$.

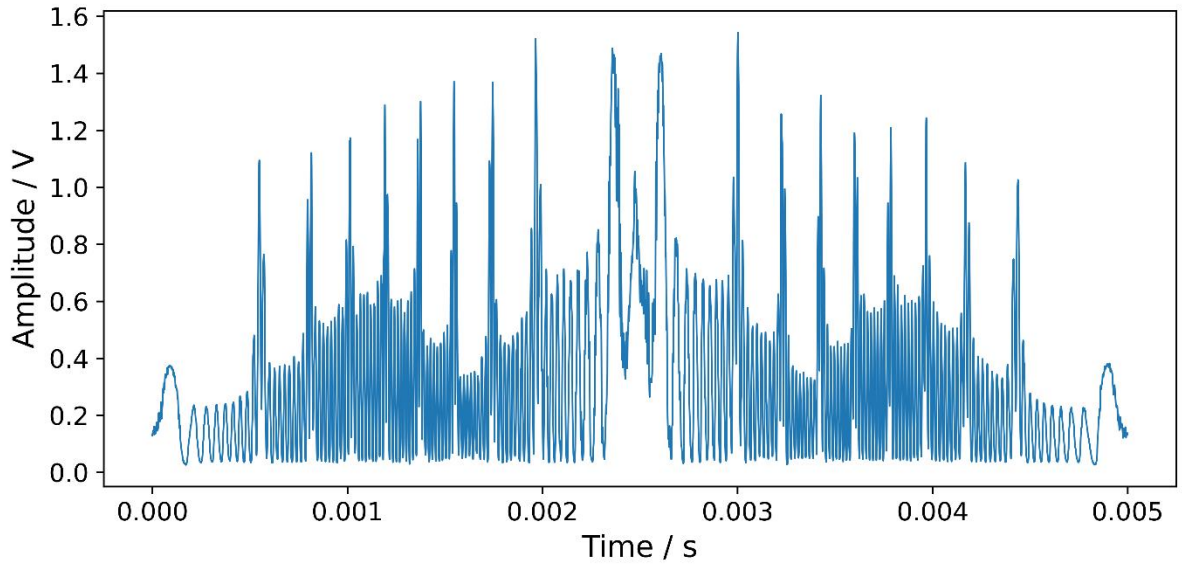

Figure 3. Photodetector signal over one modulation period.

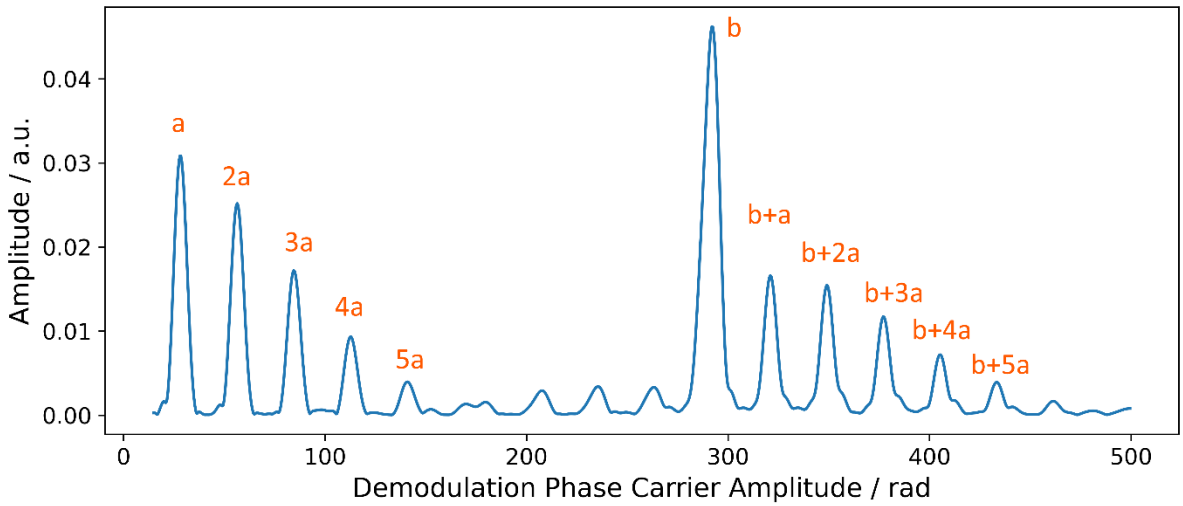

Figure 4. RRI signal amplitude as the function of demodulation phase carrier amplitude, which is proportional to OPD of the interferometer arms.

4. RESULTS AND DISCUSSION

Figure 5 shows phase changes $\Delta\varphi_i(t) - \Delta\varphi_b(t)$ evaluated for the first four multi-reflections when manually tipping the end mirror of the cavity. As can be observed, with each subsequent pass, the evaluated phase change of the induced disturbances increases, aligning with theoretical expectations. Figure 6 depicts measured displacement $\Delta a_i(t)$ as well as the averaged displacement signal. As can be seen from the image, the acquired displacement signals exhibit higher base noise levels compared to most conventional interferometers, including prior RRI [3,4] setups. This is primarily due to the use of a low-cost data acquisition board for laser wavelength modulation and photodetector signal sampling, where the ADC (Analog-to-Digital Converter) and DAC (Digital-to-Analog Converter) do not provide optimal performance. Despite this, we chose this board for its convenience, since it enables swift preparation for measurements to validate the measurement concept.

It is also observed that path b, between the fiber tip and the entry mirror of the Fabry-Perot cavity, forms a secondary cavity where multiple reflections can occur, despite it being a low-finesse cavity. These multiple reflections interfere with each other and with signal from the main Fabry-Perot cavity, forming unwanted interferences with an optical path difference (OPD) that could overlap with the evaluated signals, thus causing significant nonlinearities and additional phase noise. An example of such unwanted signals can be seen in the range view in Fig. 4 as a parasitic peaks between peaks $5a$ and b. Therefore, further investigations need to be conducted to improve the optical configuration of the interferometer. For instance, increasing the distance b, or altering it so that the interferometers formed with the reference arm result in an optical path difference (OPD) of $b + i * a$, situated between the OPD $i * a$ of direct interferences in the Fabry-Perot cavity.

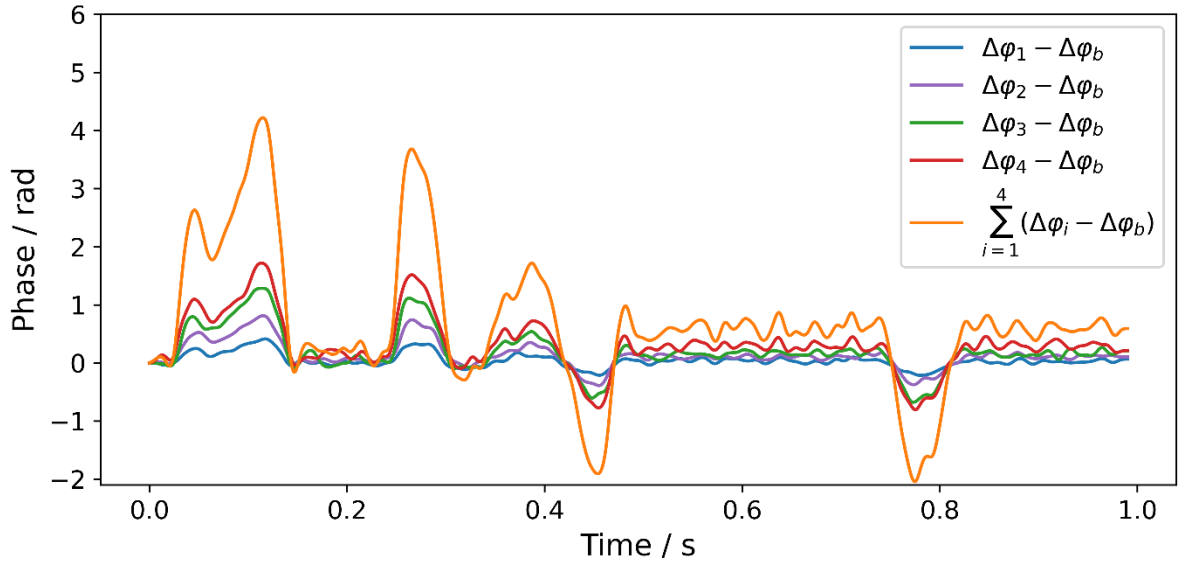

Figure 5. Phase changes $\Delta\varphi_i(t) - \Delta\varphi_b(t)$ evaluated for the first four multi-reflections when manually tipping the end mirror of the cavity.

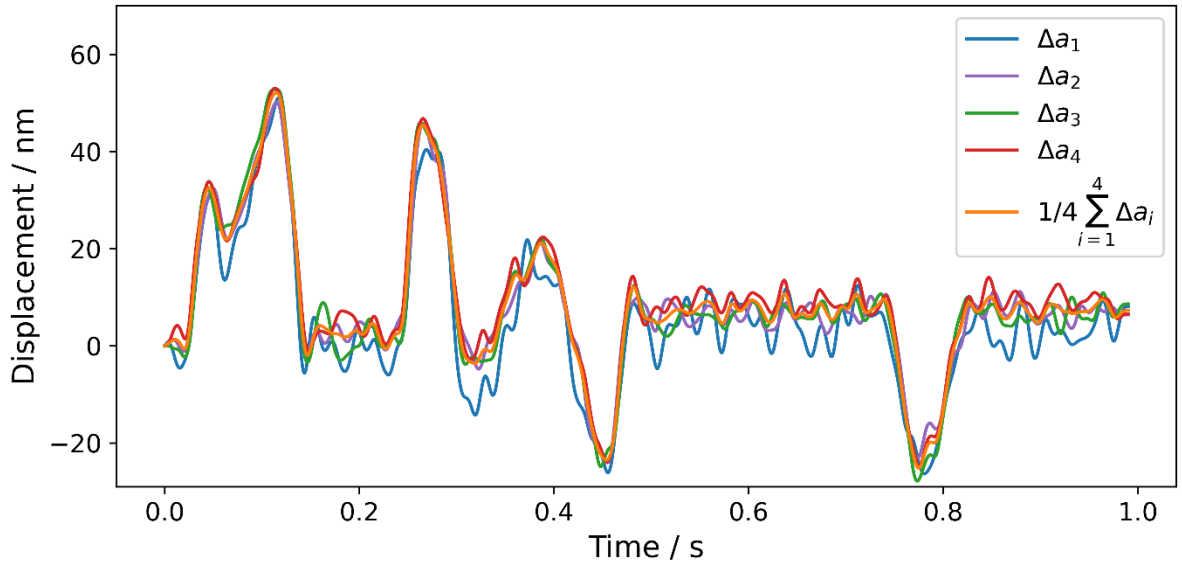

Figure 6. Displacement calculated from the phase signals.

5. CONCLUSION

This work proposes the combined use of a range-resolved interferometry method with a high-finesse Fabry-Perot setup to utilize multiple reflections in the cavity, thereby increasing the interferometer factor and, consequently, its resolution. A simple experimental proof-of-concept setup has been constructed, which allows for the evaluation of cavity length changes through the assessment of phase changes of interference signals formed by light passing through the cavity multiple times. While the experimental setup presented in this work allows for evaluating only the first four multi-reflection signals – with a noise level that is relatively high compared to conventional interferometers – it confirms the expected theory and principle of resolution enhancement through the evaluation of multiple reflections in the Fabry-Perot cavity with the RRI-method. There is potential for achieving significantly improved results through better alignment, an improved optical configuration that eliminates unwanted interferences, upgraded optical components, and advanced data acquisition system. Combined, these improvements should enable the interrogation of higher-order Fabry-Perot reflections with reduced noise. Further investigations will be conducted to explore these possible improvements.

REFERENCES

[1] Pisani M 2008 *Opt. Express* **16** 21558–21563 https://doi.org/10.1364/OE.16.021558

[2] Weichert C, Kochert P, Koning R, Flugge J, Andreas B, Kuetgens U and Yacoot A 2012 *Measurement Science and Technology* **23** 094005 https://doi.org/10.1088/0957-0233/23/9/094005

[3] Kissinger T, Charrett T and Tatam R P 2015 *Opt. Express* **23** 9415–9431 https://doi.org/10.1364/OE.23.009415

[4] Wiseman K B, Kissinger T and Tatam R P 2021 *Optics and Lasers in Engineering* **137** 106342 https://doi.org/10.1016/j.optlaseng.2020.106342

[5] Kissinger T, Correia R, Charrett T O H, James S W and Tatam R P 2016 *Journal of Lightwave Technology* **34** 4620–4626 https://doi.org/10.1109/jlt.2016.2530940

[6] Kissinger T, Chehura E, Staines S E, James S W and Tatam R P 2018 *Journal of Lightwave Technology* **36** 917–925 https://doi.org/10.1109/JLT.2017.2750759

[7] Shmagun V, Gerhardt U, Fr¨ohlich T, Manske E and Kissinger T 2022 *Measurement Science and Technology* **33** 125024 https://doi.org/10.1088/1361-6501/ac970a

CONTACTS

V. Shmagun — email: vitalii.shmagun@tu-ilmenau.de
ORCID: https://orcid.org/0000-0002-3343-2673

Dr.-Ing. U. Gerhardt — email: Uwe.Gerhardt@tu-ilmenau.de

Prof. Dr.-Ing. habil. E. Manske — email: Eberhard.Manske@tu-ilmenau.de
ORCID: https://orcid.org/0000-0002-1672-2978

Prof. Dr.-Ing. habil. T. Fröhlich — email: thomas.froehlich@tu-ilmenau.de
ORCID: https://orcid.org/0000-0002-6060-7248

Jun.-Prof. Dr. T. Kissinger

email: thomas.kissinger@tu-ilmenau.de
ORCID: https://orcid.org/0000-0003-1832-7143